JOURNAL of
MATERIALS and MECHATRONICS:A

e-ISSN 2717-8811
JournalMM, 2025, 6(1), 274-290
https://doi.org/10.55546/jmm.1675925

Araştırma Makalesi / Research Article

Development of Electronically Controlled Dual-Component Continuous Powder Feeder to Build Functional Graded Materials with Additive Manufacturing Process

Mehmet ERMURAT[1*], Serhat ZIBA[2]

[1*] Kahramanmaras Sutcu Imam University, Faculty of Engineering and Architecture, Department of Mechanical Engineering, Kahramanmaras, Türkiye,
ORCID ID: https://orcid.org/0000-0002-5661-2108, ermurat@ksu.edu.tr
Lutuf Mensucat A.Ş. Kahramanmaraş, Türkiye,
ORCID ID: https://orcid.org/0000-0002-9709-6285, serhatziba4605@hotmail.com

Geliş/ Received: 14.04.2025; **Revize/Revised:** 05.05.2025 **Kabul / Accepted:** 23.05.2025

ABSTRACT: Directed Energy Deposition methods allow parts to be produced in functional grades with different compositions across distinct regions. For this, there is a need for a powder feeder that allows multiple components to be fed into the process area simultaneously and in an integrated manner. In this study, a dual-component powder feeder was designed and manufactured. This electronically controlled powder feeder can feed two different powder materials at different flow rates at the same time. The performance of the powder feeder was tested with Ti6Al4V (flow rates of 5, 10, and 15 g/min), Zirconium (13, 20, and 30 g/min), and Inconel 625 (20, 50, and 75 g/min) powder materials. Following the calibration process, the minimum deviations were observed as 2.9% for Ti6Al4V at 15 g/min, 11.5% for Zirconium at 30 g/min, and 6.5% for Inconel 625 at 75 g/min. Conversely, the maximum deviations were recorded as 12.3% for Ti6Al4V at 10 g/min, 28.8% for Zirconium at 20 g/min, and 18.4% for Inconel 625 at 20 g/min. Overall, the lowest deviations occurred at the higher end of the examined flow rate range.

Keywords: Dual component powder feeder design, Direct energy deposition, Functionally graded material

*Sorumlu yazar / Corresponding author: ermurat@ksu.edu.tr
Bu makaleye atıf yapmak için /To cite this article

Ermurat, E., Ziba, S. (2025). Development of Electronically Controlled Dual-Component Continuous Powder Feeder to Build Functional Graded Materials with Additive Manufacturing Process. Journal of Materials and Mechatronics: A (JournalMM), 6(1), 274-290.

1. INTRODUCTION

In additive manufacturing methods used for fabricating components from metallic materials, sintering or melting can be performed using laser-based or electron beam energy sources. These methods are applicable not only to steel but also to lightweight materials such as titanium and its alloys, which possess high strength, wear resistance, and fatigue life—properties that make them suitable for the aerospace industry. Owing to their exceptional attributes, including high specific strength and excellent resistance to corrosion and oxidation, titanium and its alloys are increasingly utilized in the aerospace, marine, chemical, and biomedical industries (Wang and Liu, 2002; Courant et al., 1999; Altus and Konstantino, 2001; Zhu et al., 2014; Bruni et al., 2005; Ganesh et al., 2014; Wang et al., 2013; Weng et al., 2014).

Achieving the desired microstructure (e.g., grain size and morphology) and mechanical properties (e.g., strength, hardness, residual stress) in materials processed via additive manufacturing remains a significant challenge. It is well-established in the literature that complex metallurgical phenomena occur during the process, influenced by both material characteristics and processing parameters. Key factors such as powder characteristics (e.g., chemical composition, particle shape, particle size and distribution, flowability) and process parameters (e.g., laser type, spot size, laser power, scanning speed, and powder layer thickness) govern these phenomena (Gu et al., 2012; Santos et al., 2006).

Directed Energy Deposition (DED)—also known as Laser Metal Deposition (LMD), Direct Metal Deposition, or Laser Direct Manufacturing—is an additive manufacturing technique in which metal parts are fabricated in three dimensions. Unlike laser sintering or melting, in DED the powder is not pre-deposited but is instead delivered simultaneously and coaxially with the laser beam into the processing zone, enabling the layer-by-layer construction of components (Figure 1) (Mahamood et al., 2013). The powder feeding system includes a specially designed mechanism that transfers powder into the gas stream via a nozzle. A high-energy laser beam, focused through a lens, is directed along the Z-axis to the part, which is centered within the nozzle assembly. The vertical movement of the lens and powder nozzle enables control over the focal height of both the laser and powder. To form the desired geometries at each cross-section, the workpiece is moved in the X-Y plane by a computer-controlled system, while successive layers are deposited to create the final 3D object. Advanced DED systems—featuring multi-axis deposition, multiple powder feeders, and closed-loop control systems—facilitate the fabrication, coating, and repair of complex geometries with dimensional precision and reliable material integrity (Mazumder, 1995; Mazumder, 2010).

Recent advances have increasingly focused on the production of Functionally Graded Materials (FGMs), which provide a compositionally graded interface rather than an abrupt material transition, thereby improving bonding between the coating and substrate and reducing residual stresses (Weng et al., 2014; Dai et al., 1997; Fu and Bathchelor, 1998; Gu et al., 2012). Some studies have explored laser-melted graded coatings. For instance, Pei et al. (2002) successfully fabricated SiC/Ti-6Al-4V FGMs using laser melt injection. Developing a straightforward approach for multilayer coating via laser deposition is therefore imperative. A device with multiple, independently controlled powder feeding channels and precise flow control could significantly advance the field of multilayer FGM production (Weng et al., 2014).

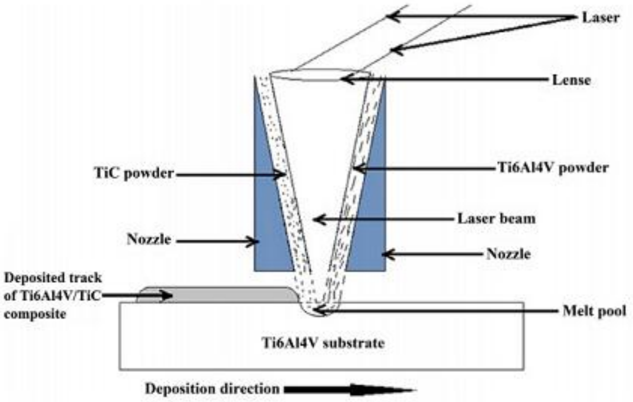

Figure 1. Directed Energy Deposition process (Mahamood RM vd. 2013)

Beyond the general capabilities of additive manufacturing, the continuous and simultaneous delivery of powder into the processing zone via the DED method enables the creation of components with spatially varying compositions.

Recent literature includes various studies on multi-material part fabrication using different additive manufacturing methods. Some employ powder bed fusion, while others utilize LMD techniques. Although many investigations focus on flat-shaped specimens, others explore the production of complex geometries. These studies generally adopt a layer-based approach, wherein material transitions occur between successive layers. They often involve the fabrication and characterization—such as microstructural analysis and mechanical testing—of metal-metal or metal-ceramic composite components (Wei et al., 2018; Wei et al., 2019; Lin and Yue, 2005; Lin et al., 2006; Li et al., 2018; Xu et al., 2015; Zhang et al., 2016; Hofmann et al., 2014).

The ability to produce point-based FGMs is a unique capability of the DED process—one not achievable through other existing additive manufacturing techniques. Realizing this functionality requires a multi-component powder feeder capable of automatically and proportionally controlling the delivery of different powder materials through independently regulated channels.

Powder control systems play a critical role in ensuring consistent and accurate delivery of powder materials by regulating key parameters such as powder quantity, flow rate, bulk density, and the ratio of mixed components. These systems are essential for maintaining process stability, material homogeneity, and overall product quality, particularly in precision-sensitive applications like additive manufacturing and pharmaceutical production. Numerous powder feeder designs exist. Screw feeders—featuring single or multiple screws—are among the most widely adopted, accommodating various powder types and sizes, and are suitable for both continuous and intermittent feeding (Engisch and Muzzio, 2015; Li et al., 2020; Blackshields and Crean, 2017; Janssen et al., 2022). In contrast, the screw-brush feeder integrates a screw for bulk transport with a rotating brush that enhances flowability and prevents bridging and aggregation, making it especially suitable for fine or easily clumping powders (Barati et al., 2015). Vibratory feeders, on the other hand, use oscillatory motion to transport and dose fragile, irregular, and cohesive powders (Singh and Chandravanshi, 2022; Wang et al., 2018).

Pump feeders operate on a simple volumetric principle, either via a cylinder-piston system that controls piston speed or via a paddle wheel system that regulates rotational speed (Besenhard et al., 2017; Mendez et al., 2012). Similarly, slide feeders are intermittent volumetric feeders that use gravity-assisted mechanisms with adjustable slides or gates to control flow—offering simplicity and reliability for handling free-flowing powders (Pohorely et al., 2004).

Fluidized feeders represent a class of systems that aerate the powder bed to achieve a fluid-like state, enhancing flowability and enabling uniform dosing. This method is particularly effective for ultrafine or cohesive powders that typically challenge conventional feeding mechanisms (Wen and Simons, 1959; Annamalai et al., 1992; Suri and Horio, 2009; Özdemir, 2009; Hou, 2024). Each type of feeder presents unique operational characteristics; the optimal choice depends on powder properties, required feed accuracy, and the specific application.

In DED additive manufacturing and cladding applications—where continuous powder feeding is essential—fluidized powder feeder types offer particularly suitable solutions due to their stable delivery characteristics. Another approach combines vibration and carrier gas flow to regulate powder delivery through gravity via an orifice. A schematic representation of such a powder feeder, presented in earlier work, is shown in Figure 2 (Ermurat, 2009), where a similar design was employed. The powder flow rate is regulated by adjusting the opening of a valve at the feeder outlet.

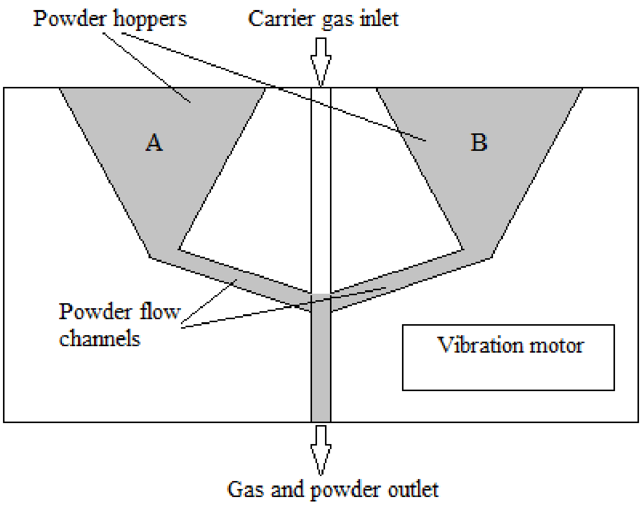

Figure 2. Schematic of Dual Component Powder Feeder (Ermurat M, 2009)

The powder feeder developed for laser metal deposition applications is capable of delivering both metallic and ceramic powders. In applications involving ceramic coatings on steel substrates, the ratio of ceramic to metallic powders varies across layers. As the deposition progresses, the ceramic content increases, culminating in a final layer composed entirely of ceramic material. This compositional gradient ensures stronger and more homogeneous bonding between the coating and substrate. Accordingly, a dual-component powder feeder is essential to achieve such gradation.

As a critical component of laser metal deposition systems, the powder feeder must fulfill specific functional requirements. The system offers an adjustable powder flow rate, a controllable carrier gas flow rate, and the ability to deliver two distinct powder types at specified ratios—with all adjustments performed manually.

In addition to its dual-component design, the powder feeder must incorporate automated control to enable efficient FGM fabrication. Although mechanical adjustment of powder flow is possible, it poses challenges in terms of precision and responsiveness. In contrast, computer-controlled systems allow more accurate and rapid regulation.

Despite the growing number of studies on multi-material additive manufacturing and functionally graded components, there remains a significant gap in the development of compact, low-cost, and semi-automated dual-component powder feeding systems specifically tailored for DED applications. Existing feeders are often either overly sophisticated and cost-prohibitive or lack the precision and flexibility needed for real-time compositional gradation. Furthermore, most systems rely on manual adjustment mechanisms, which compromise repeatability and limit point-wise material gradient control. Therefore, a versatile and accessible powder feeding system capable of accurate, simultaneous regulation of multiple powder streams is urgently needed to support the fabrication of complex FGM structures.

In response to this gap, the present study developed and implemented a dual-component, semi-automated powder feeder using the Arduino programming platform.

2. MATERIALS AND METHODS

The operating principle of the dual-component powder feeder is based on the opening of valves located beneath the powder hoppers, allowing powders to flow—assisted by vibration—into a powder transport channel. Within this channel, the powder is accelerated by a carrier gas and expelled through distribution channels at the bottom of the feeder. The valve shaft is cylindrically shaped and operates via a rotational motion driven by a stepper motor, which adjusts the opening by aligning a slit on the adjustment shaft.

The valve mechanism designed in this study adjusts the powder flow by altering the cross-sectional area of the opening as the adjustment shaft rotates. The valve shaft with some dimensions and attached O-rings is depicted in Figure 3.

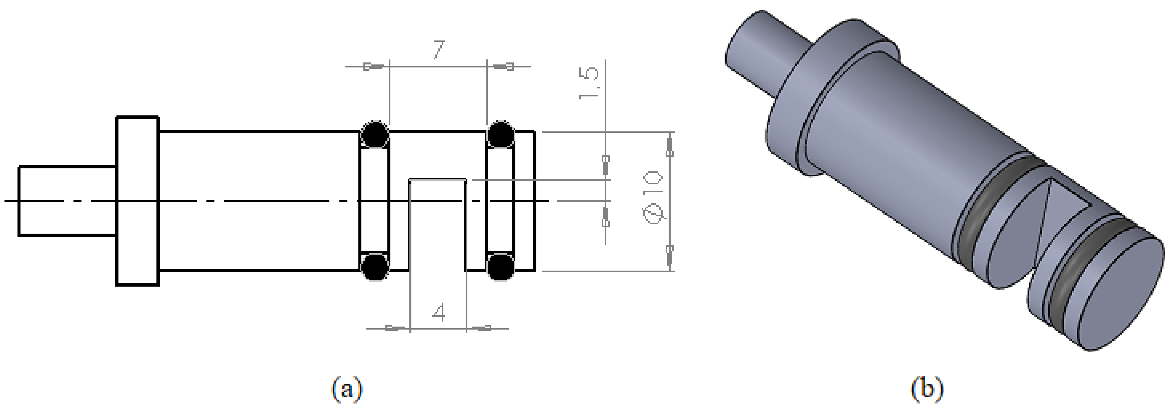

Figure 3. Valve Shaft a) front view with some dimensions b) perspective of 3D model

In Figure 4, the valve shaft is shown connected to the stepper motor via a coupling, allowing rotation. Figure 4 also presents a cross-sectional view of how the shaft is mounted on the feeder body, which is a revised version of the previous design (Figure 2), now equipped with a stepper motor to control powder flow.

When the valve adjustment shaft is aligned parallel to the feeder body channel, the valve is considered fully open, as depicted in the figure. Rotation of the adjustment shaft regulates the amount of powder being dispensed. A completely closed position corresponds to a 0% valve opening.

The vibration motor, carrier gas inlet, and valve adjustment motor are mounted on the aluminum body of the powder feeder. The internal powder flow channel follows the direction of gravity, and the mass flow rate is regulated via the valve.

Vibration is a crucial parameter in powder flow, as it reduces inter-particle friction and facilitates smoother movement. The vibration motor, mounted horizontally, employs an eccentric mass that shifts its center of gravity during rotation, thereby producing vibrational motion. The horizontal alignment of the motor enhances vertical particle movement, promoting better flowability.

The opening and closing of the stepper motors that drive the valve shaft, carrier gas, and vibration motor are all controlled automatically using the Arduino programming platform.

Due to the typically low quantities of powder fed into these systems, maintaining precise control over the feed rate is imperative for achieving reliable material deposition and process stability. Therefore, the control system must be capable of performing calculations based on user-input mass flow rates. The stepper motor is controlled via the Arduino platform.

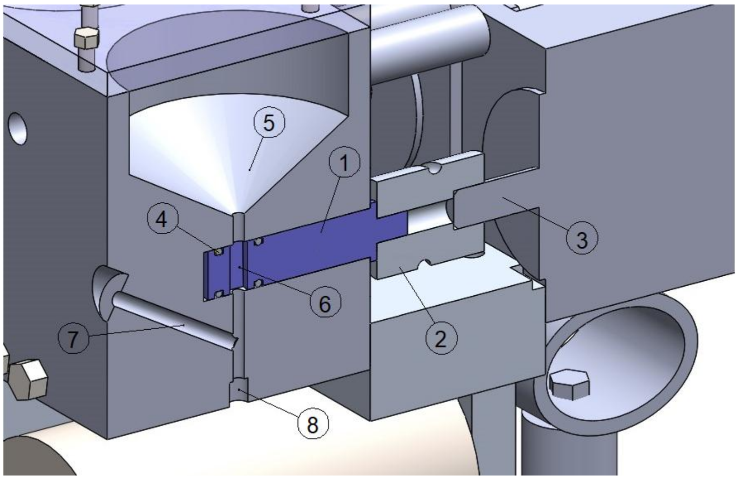

1. Valve shaft
2. Coupling
3. Stepper motor shaft
4. O-ring
5. Powder hopper
6. Shaft opening channel
7. Carrier gas channel
8. Powder feeding channel

Figure 4. Valve adjusting shaft assembly

A photograph of the fully assembled powder feeder is shown in Figure 5.

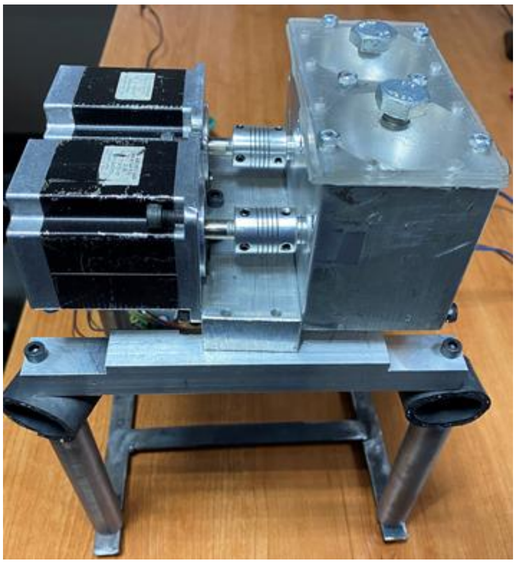

Figure 5. Dual Component Powder Feeder

To ensure rapid and accurate adjustment of powder mass flow rates, manual measurements are incorporated into an automated control system. The Arduino platform is used to perform the necessary calculations and adjustments. The control schematic of the designed powder feeder is illustrated in Figure 6, and the corresponding algorithm is provided in Figure 7.

As indicated in the flowchart of Figure 7, calibration must first be performed to determine the flow rate corresponding to specific valve shaft angles. Measurements are required at 25%, 50%, 75%, and 100% valve openings. A function must then be established to relate the valve opening to the flow rate, allowing for intermediate values to be interpolated and matched with appropriate stepper motor angles. Since the powder feeding channel is a cylindrical hole, each valve opening corresponds to a variable circular cross-sectional area. Therefore, a third-degree polynomial function has been employed to accurately model the relationship. Given the availability of four data points, this function provides a suitable fit for precise calibration, yielding a coefficient of determination of one, which denotes a perfect fit to the data and ensures an accurate representation of the relationship between flow rate and valve opening.

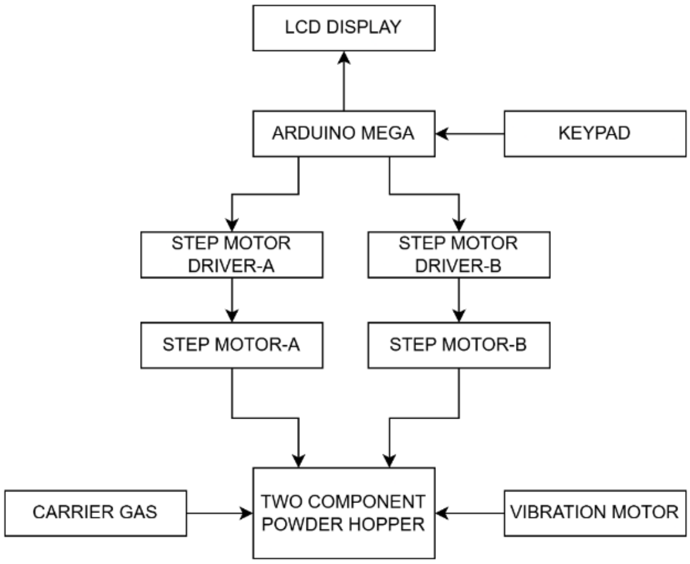

Figure 6. The powder feeder control schematic

Interpolation refers to the mathematical process of estimating unknown intermediate values of a continuous function based on a finite set of known data points. The objective is to construct a function *f(x)* that passes through these known points and can reliably predict values at locations where data is not explicitly available. This process is critical in numerical analysis and engineering applications, particularly when experimental or computational constraints prevent the acquisition of continuous data.

Various interpolation techniques are employed depending on the nature and distribution of the data points. When the known data points are not equally spaced, methods such as Lagrange interpolation or Newton's divided difference are commonly used (Burden and Faires, 2011). For equally spaced data, finite difference methods such as Newton-Gregory forward or backward interpolation are more efficient. The chosen interpolation model—whether polynomial, spline-based, or piecewise—directly affects the accuracy and smoothness of the estimated function.

In the context of additive manufacturing or mechatronic systems, interpolation functions are often utilized to calibrate or model relationships between system inputs (e.g., valve opening angles) and outputs (e.g., powder flow rates), especially when real-time sensor measurements are not feasible.

Due to the potential variation in initial valve opening positions with each run and the cylindrical cross-sectional area of the powder feeding channel, the resulting calibration data points are not uniformly spaced.

Consequently, Lagrange interpolation is employed in this study to construct a fitting polynomial that accurately represents the nonlinear relationship between the valve opening and the powder flow rate. By using a Lagrange interpolation polynomial, the model does not require equally spaced data points, thereby accommodating the inherent variability in the valve's initial positioning and ensuring reliable performance of the control algorithm.

If a parabolic interpolation in the form of $f(x) = a + a x + a x^2$ is to be performed using Lagrange polynomials based on data points such as (*x0,f0*), (*x1,f1*) and (*x2,f2*), the coordinates of these points are substituted into Equation 1 to construct a system of equations.

$$\begin{aligned} f_0 &= a_0 + a_1 x_0 + a_2 {x_0}^2 \\ f_1 &= a_0 + a_1 x_1 + a_2 {x_1}^2 \\ f_2 &= a_0 + a_1 x_2 + a_2 {x_2}^2 \end{aligned} \tag{1}$$

The coefficients of the resulting polynomial *f(x)* are then obtained by solving this system and are presented in Equation 2.

$$\begin{aligned} a_0 &= \frac{f_0(x_1 {x_2}^2 - x_2 {x_1}^2) + f_1(x_2 {x_0}^2 - x_0 {x_2}^2) + f_2(x_0 {x_1}^2 - x_1 {x_0}^2)}{(x_0 - x_1)(x_0 - x_2)(x_2 - x_1)} \\ a_1 &= \frac{f_0({x_1}^2 - {x_2}^2) + f_1({x_2}^2 - {x_0}^2) + f_2({x_0}^2 - {x_1}^2)}{(x_0 - x_1)(x_0 - x_2)(x_2 - x_1)} \\ a_2 &= \frac{f_0(x_2 - x_0) + f_1(x_0 - x_2) + f_2(x_1 - x_0)}{(x_0 - x_1)(x_0 - x_2)(x_2 - x_1)} \end{aligned} \tag{2}$$

In this case, the parabolic equation is rearranged for *f0*, *f1*, and *f2*, as shown in Equation 3.

$$f(x) = L_0 f_0 + L_1 f_1 + L_2 f_2 \tag{3}$$

The magnitudes of *Li* here are given by Equation 4, and these magnitudes are referred to as Lagrange polynomials (Yükselen, 2008).

$$L_k = \frac{(x - x_0)(x - x_1)\ldots(x - x_{k-1})(x - x_{k+1})\ldots(x - x_n)}{(x_k - x_0)(x_k - x_1)\ldots(x_k - x_{k-1})(x_k - x_{k+1})\ldots(x_k - x_n)} = \prod_{\substack{j=0 \\ j \neq k}}^{n} \frac{x - x_j}{x_k - x_j} \tag{4}$$

Consequently, curve fitting was performed using a third-degree polynomial function, $f(x)=a+ax+ax^2+ax^3$, which offers greater accuracy than lower-degree polynomials.

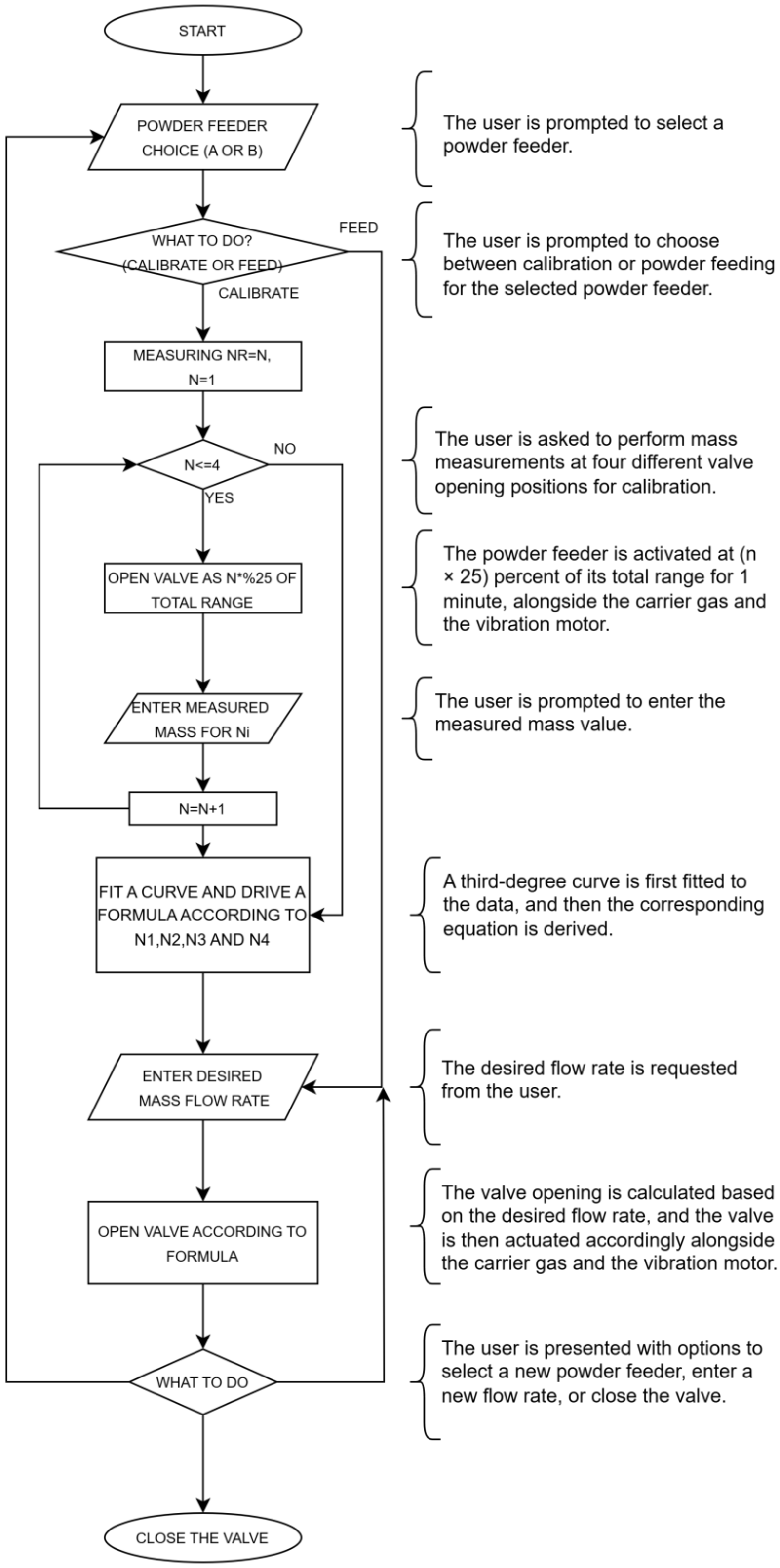

Figure 7. Algorithm of the powder feeder working

An Arduino code was developed in accordance with the algorithm illustrated in Figure 7. This implementation utilizes user-defined flow rate values corresponding to known valve opening ratios to perform polynomial regression, thereby generating a mathematical function. The resulting function enables precise calculation of the required valve opening to achieve any desired flow rate, and based on this calculation, the stepper motors are adjusted to the appropriate position, rotating the valve shaft accordingly.

All experiments conducted during both the calibration and feeding stages were repeated three times, and the average values were used for all calculations. In both stages, the valve shaft was kept open for a predetermined time interval, during which the discharged powder was collected in a clean container and weighed using a precision balance. The corresponding mass flow rates were then calculated using the standard mass flow rate equation.

Following the completion of the calibration process, three target mass flow rates were defined for each material. Based on the calibration data, the powder feeder was adjusted to determine the appropriate valve opening corresponding to each target. During each feeding test, the powder delivered over the set time interval was collected and measured, and the resulting flow rates were calculated accordingly.

3. RESULTS AND DISCUSSION

In DED processes, the precise and continuous delivery of multiple powder materials is essential for the successful fabrication of FGMs. Since metallic and ceramic powders often differ significantly in terms of density, particle morphology, and flow behavior, a conventional single-channel feeding system is usually insufficient to ensure accurate dosing and homogeneous mixing during deposition. Therefore, a dual-component powder feeding system was developed in this study to enable the simultaneous and adjustable delivery of two distinct powders. This system was designed to support the controlled production of gradient structures by providing independent flow regulation for each powder stream. In addition, the integration of a predictive control model allowed the system to calculate appropriate valve positions based on target flow rates and material-specific characteristics. The following section evaluates the calibration procedure and feeding accuracy of this system under various operating conditions.

The calibration process was conducted using different powder materials, followed by assessments of whether the actual feeding rates matched the predicted values generated by the developed model. The results obtained from these evaluations are discussed in detail.

The powder materials used and their key properties are summarized in Table 1.

Table 1. Powder materials and their some properties

Powder Material	Particle size (μm)	Particle shape
Ti6Al4V	+109 -154	Spherical
Zirkonyum	+75 -154	Irregular
Inconel 625	+90 -154	Spherical

The microscope images of the powder materials, with their sizes and shapes specified in Table 1, are presented in Figure 8.

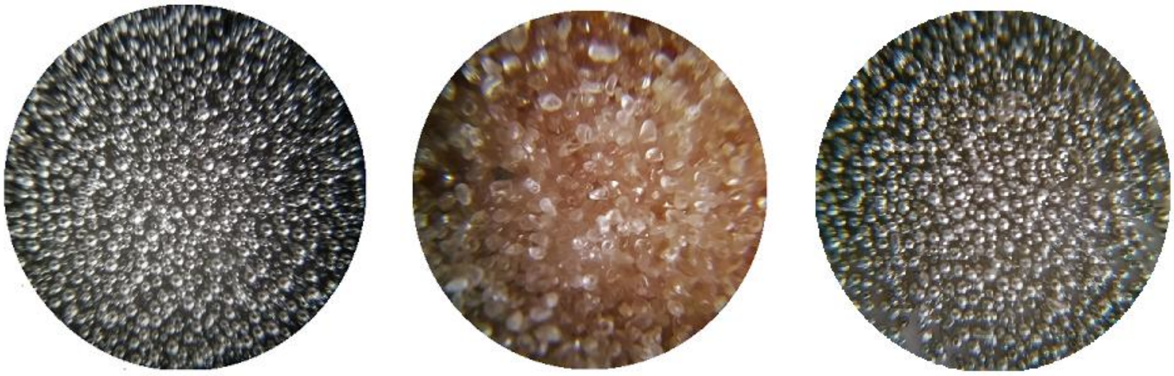

Ti6Al4V (+109-154µm) Zirconium (+75-154µm) Inconel 625 (+90-154µm)

Figure 8. Microscope images of the powder materials

Initially, calibration experiments were carried out for each powder type. Subsequently, three intermediate feed rate values were selected, and the powder feeder was commanded to calculate and adjust the valve opening angle accordingly. The amount of powder dispensed over a fixed time interval was measured, and the resulting mass flow rates were calculated. All measurements during both the calibration and the feeding phases were repeated three times for each setting, and the average values were used for analysis. In both cases, the valve was kept open for a predefined duration, during which the dispensed powder was collected in a container and weighed using a precision balance. The mass flow rate was then calculated using the standard mass flow formula. These calculations were automated via the Arduino-based control system.

Table 2 presents the average mass values obtained during calibration corresponding to valve openings of 25%, 50%, 75%, and 100% of the full opening for three powder materials.

Table 2. The average of the measurement results obtained during the calibration of the powder materials

Valve Opening	Powder flow rate (g/m)		
(%)	Ti6Al4V	Zirconium	Inconel 625
25	1,68	9,06	6,18
50	8,46	17,61	54,06
75	13,56	26,55	68,28
100	19,74	36,69	91,44

Following this, feeding was conducted at various intermediate target values, and the corresponding measurements were recorded. Table 3 presents the target values, the mean of three measurements for each case, and the relative errors for each powder material.

Table 3. Feeding results of the powder materials at the target and measured values and the resulting relative error rates

Ti6Al4V			Zirconium			Inconel 625		
Target Flowrate (g/min)	Measured Flowrate (g/min)	Rel. Error (%)	Target Flowrate (g/min)	Measured Flowrate (g/min)	Rel. Error (%)	Target Flowrate (g/min)	Measured Flowrate (g/min)	Rel. Error (%)
5	4.51	-9.8	13	11.22	-13.7	20	23.68	18.4
10	11.23	12.3	20	25.76	28.8	50	54.06	8.1
15	14.56	-2.9	30	26.55	-11.5	75	70.13	-6.5

Although the regression model demonstrates a perfect fit with the calibration dataset ($R^2 = 1$), noticeable discrepancies were observed between the predicted and actual powder feed rates during operation.

These results collectively highlight the influence of particle size, shape, and target flow rates on the precision of the feeding system, underscoring the need for material-specific calibration strategies in powder-based manufacturing processes. These deviations are primarily attributed to the inherent complexity and dynamic behavior of powder flow systems, rather than deficiencies in the mathematical model itself.

Among the tested powders, Ti6Al4V powder exhibited the lowest relative error across all target flow rates, followed by Inconel 625 powder, while Zirconium showed the highest deviations. As summarized in Table 1, Ti6Al4V and Inconel 625 exhibit spherical morphology, which is known to promote stable and predictable flow. Furthermore, Ti6Al4V powder possesses the narrowest size distribution among them. In contrast, Zirconium has angular, irregularly shaped particles with a somewhat broader size distribution, likely contributing to increased flow variability and feeding errors.

These results support the widely acknowledged view that particle shape and size distribution significantly influence flow behavior in powder feeders. Spherical particles, due to their reduced interlocking and lower surface area-to-volume ratio, generally experience less resistance during flow and are less susceptible to arching and bridging phenomena. This characteristic facilitates smoother transport through constricted geometries such as valves and funnels, leading to more consistent delivery rates—an observation consistent with the superior performance of Ti6Al4V.

On the other hand, irregular particles, like those of Zirconium, tend to interlock and form unstable flow patterns, particularly at lower feed rates. Irregular particles not only cause interlocking among themselves, but also induce flow disturbances due to the interaction between the particle and the flow path, especially around sharp features such as the valve shaft. This behavior aligns with the findings of Barati et al. (2015), where significant fluctuations in mass flow rate were observed due to powder cohesion and particle-wall interactions.

Wang et al. (2018) and Besenhard et al. (2017) also have shown that fine and cohesive powders are particularly prone to erratic flow due to agglomeration, inter-particle adhesion, and arching effects, which reduce flow reproducibility even under seemingly controlled conditions. Besenhard et al. (2017) also concluded that flow fluctuations are more likely at low feed rates due to the high surface-to-volume ratio. Similar to these findings, lower flow fluctuations were observed at higher target flow rates for each powder in this study, as presented in Table 3.

Studies by Pohorely et al. (2004) and Annamalai et al. (1992) underscore that low-rate feeding systems are particularly sensitive to small disturbances in powder behavior, especially under micro-feeding regimes. These physical phenomena introduce nonlinearities and disturbances that are not captured by regression models trained on static datasets.

These insights underscore the importance of integrating material-specific considerations into the design and calibration of powder feeding systems. For instance, in applications involving powders with poor flowability—like Zirconium—strategies such as vibrational agitation, assisted gas flow, and optimized flow channel geometry should be precisely tuned to stabilize the feed. This is supported by Mendez et al. (2012), who showed that feed frame geometry and dynamic interactions between powder and wall surfaces can drastically affect feed uniformity.

Therefore, while the regression model provides an idealized estimation of the valve position required to achieve a target flow rate, real-time deviations stem predominantly from transient flow instabilities, batch-to-batch material variability, and mechanical limitations of the feeder hardware—all of which are well-documented challenges in the field of powder technology (Blackshields and Crean, 2017; Engisch and Muzzio, 2015; Janssen et al., 2022).

In summary, the deviations observed in Table 3 are not merely the result of mechanical limitations but reflect the complex interplay between powder shape, size, cohesion, and the chosen feeding method. These findings highlight the need for adaptive and material-aware control strategies in dual-channel powder feeders, particularly when dealing with non-spherical or fine-grained powders.

The dual-channel powder feeder developed in this study provides a robust and adaptable foundation for the implementation of FGM strategies via DED, particularly in high-performance components such as compressor disks and turbine blades. These components must withstand extreme thermal loads, high rotational speeds, and severe wear conditions—especially in the case of compressor disks, where both fatigue and surface degradation due to abrasion pose significant operational risks (Aschenbruck J et al.,2014). The ability to precisely regulate and independently deliver different powder materials enables tailored material gradients, which significantly enhance resistance to mechanical and thermal stresses. This flexibility, combined with the automatic control of variable feed rates for dual powder materials, makes such a powder feeder particularly valuable for the production of performance-critical components—especially in defense, aerospace, and energy sectors—through FGM strategies implemented via DED additive manufacturing (Nazir A et al., 2023).

4. CONCLUSION

This study introduced a novel dual-component powder feeding system designed to enable independent flow control for each powder line in DED applications. The system integrates a calibration-based predictive model that determines the appropriate valve position for a target flow rate based on the feeding characteristics of each powder type. The proposed method was validated through a series of calibration and controlled feeding experiments using Ti6Al4V, Inconel 625, and Zirconium materials. Based on the results obtained, the following conclusions can be drawn:

- Each material was fed at selected target flow rates, and the achieved values were compared against predicted outputs to evaluate the system's accuracy.
- The minimum relative deviations were observed as 2.9% for Ti6Al4V at a flow rate of 15 g/min, 11.5% for Zirconium at 30 g/min, and 6.5% for Inconel 625 at 75 g/min. Conversely, the maximum deviations were recorded as 12.3% for Ti6Al4V at 10 g/min, 28.8% for Zirconium at 20 g/min, and 18.4% for Inconel 625 at 20 g/min. In general, lower deviations were observed at higher flow rates.
- Ti6Al4V powder exhibited the lowest relative error across all target flow rates due to its spherical morphology and narrow size distribution. Conversely, Zirconium powder exhibited the highest relative error, primarily due to its irregular morphology and broader particle size distribution.
- The mass flow behavior of powders was fundamentally governed by material-specific physical properties, especially density and particle morphology, under gravity-driven feeding conditions. For instance, Inconel 625, with its substantially higher density, exhibited the highest mass flow rate among all tested powders. This aligns with the literature emphasizing

the dominant influence of gravitational forces in free-flow feeding systems (Engisch and Muzzio, 2015; Annamalai et al., 1992).

- Despite the irregular morphology of Zirconium powder—which is commonly associated with poor flowability—the presence of finer particles in its distribution appeared to enhance its flow behavior. As a result, Zirconium outperformed Ti6Al4V in terms of mass flow rate under comparable conditions, underscoring the compensatory role of particle size over shape (Barati Dalenjan et al., 2015; Janssen et al., 2022).
- The favorable flow performance of Inconel 625 was further enhanced by its spherical particle shape, which minimized inter-particle friction and supported a more streamlined flow through the valve opening. Additionally, its relatively narrow particle size distribution enabled higher volumetric fill and more uniform movement through the feeder system, consistent with findings in Besenhard et al. (2017) and Wang et al. (2018).
- Polynomial regression modeling enabled precise calibration of the relationship between valve opening and powder mass flow rate. The calibration curve, established via third-order polynomial interpolation based on four data points, exhibited a perfect fit ($R^2 = 1.000$). However, deviations observed in actual feed performance, particularly at lower valve openings, indicate that such models alone may not capture all dynamic effects present in real-time operations—especially in the presence of complex powder behaviors. This aligns with prior studies emphasizing that while modeling provides a foundational understanding, physical phenomena such as particle bridging, vibration-induced segregation, or refill-induced disturbances can significantly affect feeding stability (Li et al., 2020; Blackshields and Crean, 2017).
- The most pronounced deviation from predicted feed rates was observed with Zirconium, which also exhibited the largest variation across repeated measurements. This instability is attributable to its irregular particle shape and broader size distribution, which likely caused erratic flow, frequent clogging, and intermittent surges. Such behaviors are consistent with the challenges of feeding cohesive or irregularly shaped powders highlighted in Wang et al. (2018) and Pohorely et al. (2004).
- A general trend of reduced error and improved consistency was observed at higher valve openings for all powder types. This observation suggests that increased aperture reduces the relative influence of particle morphology and enhances bulk flow stability—findings that are in agreement with the work of Singh and Chandravanshi (2022), who demonstrated the positive correlation between opening size and feed uniformity in vibratory feeder systems.

In conclusion, this study confirms that the dual-channel powder feeder system is capable of delivering accurate and consistent powder flow for a variety of materials. Nevertheless, for powders with challenging flow characteristics—such as Zirconium—enhanced control strategies, including real-time feedback or active vibration mechanisms, may be necessary to mitigate fluctuations. These findings highlight the critical interplay between powder physical characteristics and mechanical feeding design, reinforcing the need for integrated approaches that combine predictive modeling with process-aware engineering solutions in future developments.

5. ACKNOWLEDGEMENTS

This study was supported by the Scientific Research Projects Unit (BAP) of Kahramanmaraş Sütçü İmam University under the project number 2019/6-12 YLS.

6. CONFLICT OF INTEREST

Authors approve that to the best of their knowledge, there is not any conflict of interest or common interest with an institution/organization or a person that may affect the review process of the paper.

7. AUTHOR CONTRIBUTION

Mehmet ERMURAT contributed to determining the concept and/or design process of the research, managing the concept and/or design process, data collection, data analysis and interpretation of the results, preparation of the manuscript, critical analysis of the intellectual content, and final approval and full responsibility. Serhat ZIBA contributed to determining the concept and/or design process of the research, data collection, data analysis and interpretation of the results, preparation of the manuscript, and final approval and full responsibility.

8. REFERENCES

Altus E., Konstantino E., Optimum laser surface treatment of fatigue damaged Ti–6Al–4V alloy. Materials Science and Engineering: A 302(1), 100–105, 2001.

Annamalai K., Ruiz M., Vo N., Anand V., Locally fluidizing feeder for powder transport. Powder Technology 73, 181–190, 1992. https://doi.org/10.1016/0032-5910(92)80079-C

Aschenbruck J, Adamczuk R, Seume J. R., Recent Progress in Turbine Blade and Compressor Blisk Regeneration, Procedia CIRP 22, 256-262, 2014. https://doi.org/10.1016/j.procir.2014.07.016.

Barati Dalenjan M., Jamshidi E., Ale Ebrahim H., A screw-brush feeding system for uniform fine zinc oxide powder feeding and obtaining a homogeneous gas-particle flow. Advanced Powder Technology 26, 303–308, 2015. https://doi.org/10.1016/j.apt.2014.10.010

Besenhard M. O., Fathollahi S., Siegmann E., Slama E., Faulhammer E., Khinast J. G., Micro-feeding and dosing of powders via a small-scale powder pump. International Journal of Pharmaceutics 519(1-2), 314–322, 2017. https://doi.org/10.1016/j.ijpharm.2016.12.029

Blackshields C. A., Crean A. M., Continuous powder feeding for pharmaceutical solid dosage form manufacture: a short review. Pharmaceutical Development and Technology 23(6), 554–560, 2017. https://doi.org/10.1080/10837450.2017.1339197

Bruni S., Martinesi M., Stio M., Treves C., Bacci T., Borgioli F., Effects of surface treatment of Ti–6Al–4V titanium alloy on biocompatibility in cultured human umbilical vein endothelial cells. Acta Biomater 1(2), 223–234, 2005.

Burden R. L., Faires, J. D., Numerical Analysis. 9th Edition, Brookscole, Boston, 259-253, 2011.

Courant B., Hantzpergue J. J., Benayoun S., Surface treatment of titanium by laser irradiation to improve resistance to dry-sliding friction. Wear 236, 39–46, 1999.

Dai Z. D., Pan S. C., Wang M., Yang S. R., Zhang X. S., Xue Q. J., Improving the fretting wear resistance of titanium alloy by laser beam quenching, Wear 213(1-2), 135–139, 1997.

Engisch W. E., Muzzio F. J., Feedrate deviations caused by hopper refill of loss-inweight feeders. Powder Technology 283, 389–400, 2015.

Ermurat M., Lazerli Doğrudan Metal Parça İmalatı Sisteminin Geliştirilmesi, Üretilen Parça Özelliklerinin İncelenmesi ve Sistem Optimizasyon, Kocaeli Üniveritesi Fen Bilimleri Enstitüsü, Doktora Tezi (Basılmış), 2009.

Fu Y. Q., Batchelor A. W., Laser nitriding of pure titanium with Ni, Cr for improved wear performance, Wear 214, 83–90, 1998.

Ganesh B. K. C., Sha W., Ramanaiah N., Krishnaiah A., Effect of shotpeening on sliding wear and tensile behavior of titanium implant alloys. Materials & Design, 56, 480–486, 2014.

Gu D. D., Meiners W., Wissenbach K., Poprawe R., Laser additive manufacturing of metallic components: materials, processes and mechanisms. International Materials Reviews, 57(3), 133-164, 2012.

Hofmann D. C., Kolodziejska J., Roberts S., Otis R., Dillon R. P., Suh J. O., Liu Z-K., Borgonia, J. P., Compositionally graded metals: A new frontier of additive manufacturing, Journal of Materials Research, 29(17), 1899-1910, 2014.

Hou P. C. H., Development of a Micro-Feeder for Cohesive Pharmaceutical Powders, PhD.Thesis, Strathclyde Institute of Pharmacy and Biomedical Sciences University of Strathclyde, Glasgow, UK, 2024,

Janssen P. H. M., Kulkarni S. S., Torrecillas C. M., Tegel F., Weinekötter R., Meir B., Dickhoff, B. H. J., Effect of batch-to-batch variation of spray dried lactose on the performance of feeders. Powder Technology. 409, 117776, 2022. https://doi.org/10.1016/J.POWTEC.2022.117776

Li J., Cheng X., Liu D., Zhang S. Q., Li Z., He B., Wang H. M. Phase evolution of a heat-treatable aluminium alloy during laser additive manufacturing. Materials Letters 214, 56-59, 2018.

Li T., Scicolone J. V., Sanchez E., Muzzio F. J., Identifying a Loss-in-Weight Feeder Design Space Based on Performance and Material Properties. Journal of Pharmaceutical Innovation 15, 482–495, 2020.

Lin X., Yue T. M., Yang H. O., Huang W. D., Microstructure and phase evolution in laser rapid forming of a functionally graded Ti-Rene88DT alloy. Acta Materialia 54(7), 1901-1915, 2006.

Lin X., Yue T. M., Phase formation and microstructure evolution in laser rapid forming of graded ss316L/Rene88DT alloy. Materials Science and Engineering: A 402, 294-306, 2005.

Mahamood R. M., Akinlabi E. T., Shukla M., Pityana S., Scanning velocity influence on microstructure, microhardness and wear resistance performance of laser deposited Ti6Al4V/TiC composite. Materials & Design 50, 656–666, 2013.

Mazumder J., Voelkel D. D., Method and apparatus for noncontact surface contour measurement. US patent no. 5446549, 1995.

Mazumder J., Morgan D., Skszek T. W., Lowney M., Direct metal deposition apparatus utilizing rapid-response diode laser source. US patent no. 7765022, 2010.

Mendez R., Velazquez C., Muzzio F. J., Effect of feed frame design and operating parameters on powder attrition, particle breakage, and powder properties, Powder Technology, 229, 253-260, 2012. ISSN 0032-5910

Nazir A, Gokcekaya O, Masum Billah K. M, Ertugrul O, Jiang J, Sun J, Hussain S, Multi-material additive manufacturing: A systematic review of design, properties, applications, challenges, and 3D printing of materials and cellular metamaterials, Materials & Design 226, 111661, 2023. ISSN 0264-1275, https://doi.org/10.1016/j.matdes.2023.111661.

Özdemir A. C., Lens'te 3 Farklı Tozu Aynı Katmana Yığma Kafası Tasarımı, Gebze Yüksek Teknoloji Enstitüsü, Mühendislik ve Fen Bilimleri Enstitüsü, Yüksek Lisans Tezi (Basılı), 2009

Pei Y. T., Ocelik V., De Hosson J. T. M., SiCp/Ti6Al4V functionally graded materials produced by laser melt injection. Acta Materialia 50(8), 2035–2051, 2002.

Pohořelý M., Svoboda K., Hartman M., Feeding small quantities of particulate solids. Powder Technology 142, 1–6, 2004. https://doi.org/10.1016/j.powtec.2004.03.005

Santos E. C., Shiomi M., Osakada K., Laoui T., Rapid manufacturing of metal components by laser forming. International Journal of Machine Tools and Manufacture 46(12-13), 1459–1468, 2006.

Singh C., Chandravanshi M. L., Dynamic analysis and performance assessment of a vibratory feeder for different motor positions on trough. Mechanics Based Design of Structures and Machines 51(11), 6453-6470, 2022. https://doi.org/10.1080/15397734.2022.2047720

Suri A., Horio M., A novel cartridge type powder feeder, Powder Technology,189(3), 497-507, 2009.

Wang H. M., Liu Y. F., Microstructure and wear resistance of laser clad Ti5Si3/NiTi2 intermetallic composite coating on titanium alloy, Materials Science and Engineering: A 338(1-2), 126–132, 2002.

Wang Q., Zhang P. Z., Wei D. B., Chen X. H., Wang R. N., Wang H. Y., Microstructure and sliding wear behavior of pure titanium surface modified by double-glow plasma surface alloying with Nb, Materials & Design, 52, 265–73, 2013.

Wang H., Wu L., Zhang T., Chen R., Zhang L., Continuous micro-feeding of fine cohesive powders actuated by pulse inertia force and acoustic radiation force in ultrasonic standing wave field. International Journal of Pharmaceutics. 545, 153–162, 2018. https://doi.org/10.1016/j.ijpharm.2018.05.006

Wei C., Li L., Zhang X., Chueh Y. H. 3D Printing of multiple metallic materials via modified selective laser melting. CIRP Annals-Manufacturing Tech, 67, 245-248, 2018.

Wei C., Sun Z., Chen Q., Liu Z., Li L., Additive Manufacturing of Horizontal and 3D Functionally Graded 316L/Cu10Sn Components via Multiple Material Selective Laser Melting. Journal of Manufacturing Science and Engineering 141(8) 081014, 2019.

Wen C. Y., Simons H. P., Flow characteristics in horizontal fluidized solids transport. AIChE Journal, 5(2), 263–267, 1959. https://doi.org/https://doi.org/10.1002/aic.690050225

Weng F., Chen C., Yu H., Research status of laser cladding on titanium and its alloys: A review. Materials and Design, 58, 412–425, 2014.

Xu W., Brandt M., Sun S., Elambasseril J., Liu Q., Latham K., Qian M., Additive manufacturing of strong and ductile Ti-6Al-4V by selective laser melting via in site martensite decomposition. Acta Materialia 85, 74-84, 2015.

Yükselen M. A, HM504 Uygulamalı Sayısal Yöntemler Ders Notları, 2008.

Zhang Y. Z., Liu Y. T., Zhao X. H., Tang Y. J., The interface microstructure and tensile properties of direct energy deposited TC11/Ti2AlNb dual alloy. Materials and Design 110, 571-580, 2016.

Zhu Y. Y., Liu D., Tian X. J., Tang H. B., Wang H. M., Characterization of microstructure and mechanical properties of laser melting deposited Ti–6.5Al–3.5Mo–1.5Zr–0.3Si titanium alloy. Materials & Design, 56, 445–453, 2014.